TU Delft

Delft University of Technology

Document Version
Final published version

Licence
Dutch Copyright Act (Article 25fa)

Citation (APA)
Koopman, C. I., Albertsma, J., van der Veen, M. A., & Vermaas, D. A. (2026). Electrochemically Mediated Separation of Carbon Monoxide Using a Ni-Based Redox Couple. *ACS Energy Letters*, *11*(2), 2229-2234. https://doi.org/10.1021/acsenergylett.5c04138

Important note
To cite this publication, please use the final published version (if applicable).
Please check the document version above.

Copyright
In case the licence states “Dutch Copyright Act (Article 25fa)”, this publication was made available Green Open Access via the TU Delft Institutional Repository pursuant to Dutch Copyright Act (Article 25fa, the Taverne amendment). This provision does not affect copyright ownership.
Unless copyright is transferred by contract or statute, it remains with the copyright holder.

Sharing and reuse
Other than for strictly personal use, it is not permitted to download, forward or distribute the text or part of it, without the consent of the author(s) and/or copyright holder(s), unless the work is under an open content license such as Creative Commons.

Takedown policy
Please contact us and provide details if you believe this document breaches copyrights.
We will remove access to the work immediately and investigate your claim.

This work is downloaded from Delft University of Technology.

ACS Energy LETTERS

http://pubs.acs.org/journal/aelccp

Letter

Electrochemically Mediated Separation of Carbon Monoxide Using a Ni-Based Redox Couple

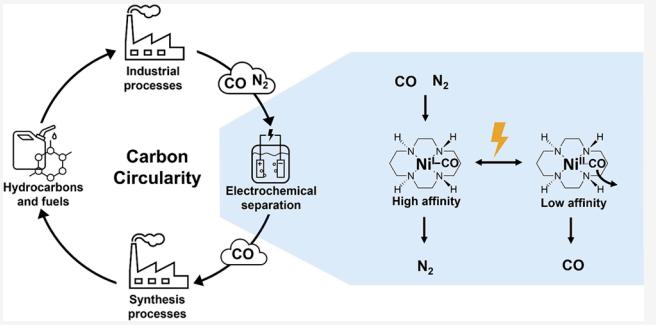
Christel I. Koopman, Jelco Albertsma, Monique A. van der Veen, and David A. Vermaas*

Cite This: *ACS Energy Lett.* 2026, 11, 2229−2234

Read Online

ACCESS | Metrics & More | Article Recommendations | Supporting Information

ABSTRACT: Carbon monoxide in industrial waste gases is often burned and is responsible for about 8% of industrial CO_2 emissions. In contrast to CO_2 capture, no conventional technologies are available for separating CO from nitrogen at scale. Here, we show that the difference in the CO binding affinity between $[Ni^{I}(cyclam)]^{+}$ and $[Ni^{II}(cyclam)]^{2+}$ can be leveraged in an electrochemical separation method: cycled capture and release of CO through potential control. The carrier, $[Ni^{I}(cyclam)]^{+}$, has a binding constant with CO that was estimated to be 7×10^{3} M^{-1} through the deconvolution of cyclic voltammetry curves. An electroswing between −1.7 V and −1.5 V vs ferrocene is sufficient to switch between the capture and release of CO. A more positive release potential can increase the release rate of CO albeit at the expense of the current efficiency. This work shows that a $[Ni(cyclam)]Cl_2$ carrier can selectively separate and concentrate CO from nitrogen electrochemically.



Carbon circularity is important to maintain sustainable CO_2 levels in the atmosphere and decrease our reliance on fossil fuels to produce carbon-based chemicals and fuels. Recycling of carbon monoxide (CO) can contribute largely to this circularity, as CO is both an essential feedstock for the chemical industry (e.g., Fischer−Tropsch, methanol synthesis, and metallurgy) and at the same time a major component in industrial waste gases, such as from blast furnaces in the steel industry.[1−3] Studies have estimated that recycling of CO from the steel industry would reduce the CO_2 emissions from industry by about 8%, which is equivalent to a reduction in total man-made CO_2 emissions of 1−2%.[3−5] Recycling 77% of CO from the European steel industry would be more than sufficient to provide the total demand for methanol and ethanol production in Europe,[3] and similar results are expected for other regions. However, this potential feedstock is currently lost through the combustion of CO-containing waste gases for energy generation, converting and emitting the CO as CO_2 into the environment. This is because separating CO from mixed gases proves challenging due to similar physical properties, especially between CO and nitrogen (e.g., molecular weight, boiling point, and kinetic diameter), making conventional separation methods inefficient and/or energy-intensive.[4,6] Thus, the carbon circularity of CO requires a new separation method.

A property to exploit for CO/N_2 separation is the affinity of CO to form π-complexation bonds. Coordination between transition metals and CO involves σ-donation of electrons from the CO ligand to the metal and π-backbonding from the metal to the π^*-antibonding orbital of the CO. Generally, electron-rich metals in their lower oxidation state are more capable of π-backbonding.[7] This is illustrated by the hemoglobin in our blood, where CO binds strongly to Fe^{2+} sites but has no binding affinity to Fe^{3+} (in methemoglobin).[8] This difference in binding affinity, dependent on the oxidation state of transition metals, is something that we leverage to develop an electrochemical separation process for CO.

Compared with conventional separation methods that rely on thermal or mechanical driving forces, electrochemically mediated sorption could offer improved energy efficiencies. The regeneration energy can selectively be supplied to the active site for separation while providing the opportunity to operate at ambient temperatures and produce a high-pressure product stream.[9−11]

A suitable electroactive carrier for CO separation is electrochemically switchable and has a different binding affinity in its two oxidation states. This results in the binding of CO in one oxidation state and the release of CO (as CO) in the other oxidation state. For practical applications, we want to operate in a system that is resilient to water and can reach acceptable carrier concentrations. Here, we present $[Ni(cyclam)]Cl_2$ as a redox-switchable carrier for CO separation.

Received: December 12, 2025
Revised: January 5, 2026
Accepted: January 6, 2026
Published: January 19, 2026



Downloaded via TU DELFT on February 25, 2026 at 14:54:58 (UTC).
See https://pubs.acs.org/sharingguidelines for options on how to legitimately share published articles.

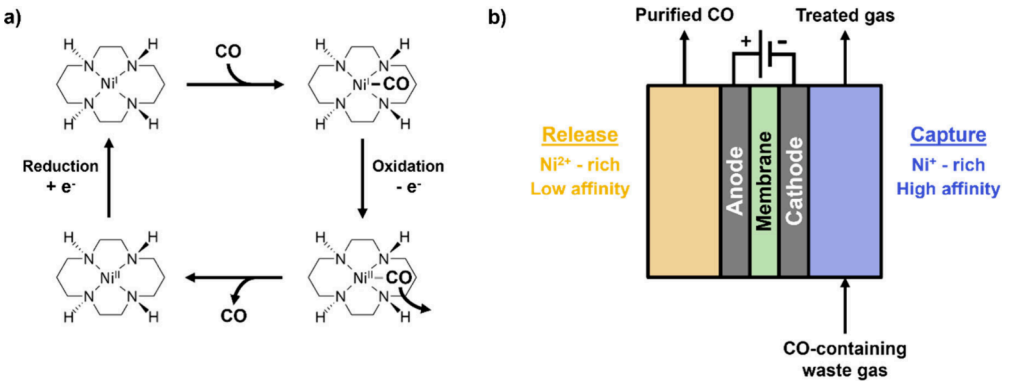


Figure 1. Electrochemically mediated absorption of carbon monoxide with a Ni(cyclam) carrier. (a) Activation and regeneration of the carrier through redox reaction. (b) Schematic representation of the electrochemically mediated separation process using electrochemistry to regenerate and activate the carrier material.

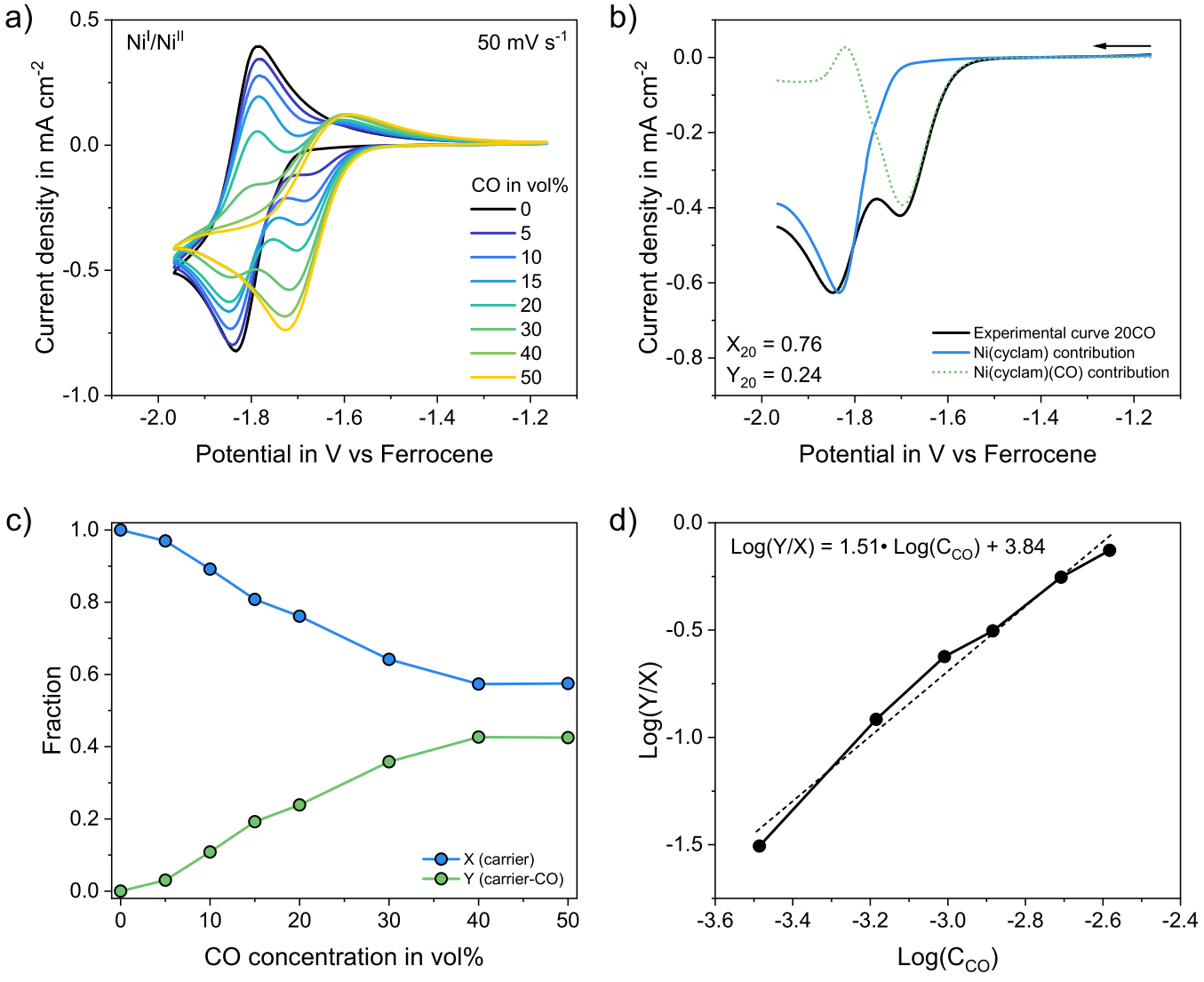


Figure 2. (a) Cyclic voltammetry measurements of the $[Ni^{I}(cyclam)]^{+}/[Ni^{II}(cyclam)]^{2+}$ redox couple (Ni^{I}/Ni^{II} in figure) under N_2 and CO environments. The electrolyte solution is 5 mM $[Ni(cyclam)]Cl_2$ and 0.1 M $TBAPF_6$ in 4:1 acetonitrile−water mixture. The solution is sparged with 2 mL min^{-1} of gas at 1.09 bar, ranging from 0 to 50 vol % CO in N_2. The scan rate is 50 mV s^{-1}. (b) Deconvolution of the cathodic scan of the 20 vol % CO cyclic voltammetry curve. The Ni(cyclam)CO contribution represents the 20CO curve after subtracting the Ni(cyclam) contribution. X_{20} and Y_{20} represent the distribution fractions of the carrier without and with CO, respectively. (c) Distribution fractions of the unbound and CO-bound carrier plotted against the feed CO concentration. (d) Hill plot of the carrier−CO equilibrium.

https://doi.org/10.1021/acsenergylett.5c04138
ACS Energy Lett. 2026, 11, 2229−2234

$[Ni(cyclam)]Cl_2$ has been used as a molecular catalyst for electrochemical CO_2 reduction to CO but exhibits deactivation through strong binding between CO and $[Ni^I(cyclam)]^+$.[12,13] Although this property is troublesome for CO_2 reduction, it makes $[Ni(cyclam)]Cl_2$ a potential carrier material for CO absorption. Naturally, the carrier should also be able to release the CO, which we hypothesize should be realized by oxidizing the carrier. This way, CO can be separated through electrochemically mediated absorption (Figure 1). We used cyclic voltammetry to study the binding affinity of the carrier and performed capture and release experiments in an H-cell.

Cyclic Voltammetry to Study the Carrier's Binding Affinity

To assess the suitability of the redox couple for electrochemical CO separation, we performed cyclic voltammetry measurements equilibrated to mixed gas of N_2, CO_2, and CO (SI-2), representing the composition of blast furnace gas in steel manufacturing (Table S1). Interaction between the CO and the redox couple should shift the cyclic voltammetry to a different reduction potential. The preferential coordination of CO to the transition metal in its lower oxidation state will move the standard redox potentials to more positive potentials through stabilization of the lower oxidation state compared to the higher oxidation state and was observed earlier in CV measurements of $[Ni(cyclam)]Cl_2$, Cu-complexes, and metal-porphyrins with CO.[12,14−16] Our CV measurements of the $[Ni(cyclam)]Cl_2$ carrier also demonstrate this shift of the standard reduction potential toward more positive potentials when increasing the CO concentration in a N_2 environment (Figure 2a).

The $[Ni^I(cyclam)]^+/[Ni^{II}(cyclam)]^{2+}$ redox couple exhibits a reduction and oxidation peak around −1.8 V vs ferrocene under a N_2 environment. The addition of CO introduces a reduction peak at −1.7 V vs ferrocene and a small oxidation peak at −1.6 V vs ferrocene. With increasing CO partial pressure, the peak at −1.8 V decreases while the new reduction peak at −1.7 V increases. We hypothesize that the redox couple at −1.8 V represents the Ni(cyclam) species without CO, while the peaks at −1.7 and −1.6 V represent the redox couple with a CO bound to the Ni-site, $[Ni^I(cyclam)(CO)]^+$. Due to the equilibrium between the CO-bound and unbound Ni(cyclam) species, both redox species exist for low CO concentrations and cause two peaks in the CV.

The half-wave potential of the $[Ni^I(cyclam)]^+/[Ni^{II}(cyclam)]^{2+}$ redox couple has shifted toward more positive potentials by 0.15 V under a CO environment, indicating improved stability of the lower oxidation state through coordination with CO. This shift is close to the reported value in the literature, of 0.17 V.[17] A shift of 0.15 V can be translated to a change in Gibbs energy of −15 kJ mol^{-1} of the $[Ni^I(cyclam)]^+/[Ni^{II}(cyclam)]^{2+}$ redox couple upon binding to CO through the relation between Gibbs free energy and potential difference ($-\Delta G = nF\Delta E$). DFT calculations for the two predominant isomers, *Trans I* and *Trans III*, also show a stronger binding of CO to the $[Ni^I(cyclam)]^+$ oxidation state, with a difference in Gibbs free energy between $[Ni^I(cyclam)]^+$ and $[Ni^{II}(cyclam)]^{2+}$ of about 40 kJ mol^{-1} (Table 1).

Additionally, the presence of CO results in a smaller oxidation peak, implying a reduced reversibility of the $[Ni^I(cyclam)(CO)]^+$ species. This could be caused by slower kinetics of the oxidation reaction when CO is coordinated to the Ni^I metal site and suggests that the rate of release of CO will be slow compared to capture.

Table 1. Change in Gibbs Energy in kJ mol^{-1} for the Binding of CO to Ni(cyclam) Trans I and Trans III Obtained from DFT Calculations

	Trans I	Trans III
$[Ni^0(cyclam)]$	−169	−181
$[Ni^I(cyclam)]^+$	−34	−29
$[Ni^{II}(cyclam)]^{2+}$	6	11

The $[Ni^{II}(cyclam)]^{2+}/[Ni^{III}(cyclam)]^{3+}$ redox couple shows no significant changes between the N_2 and the CO environments (Figure S5), making this oxidation state couple ineffective for electrochemical CO separation. Additionally, it is imperative to avoid reduction of Ni^I to Ni^0 due to the potentially irreversible generation of highly toxic $Ni^0(CO)_4$ (SI-4). We warn researchers that small amounts of highly toxic $Ni(CO)_4$ can be generated during the reduction of Ni complexes in the presence of CO.

CV Deconvolution for Binding Constant and Carrier Capacity Determination

To estimate the binding constant and number of CO molecules bound to a single carrier, we deconvolute the CV curves at different CO concentrations by the contribution of Ni(cyclam) and Ni(cyclam)(CO) using the 0 and 50 vol% CO curves. The unbound and CO-bound carrier contributions for the 5−30 vol% CO curves can be estimated from fitting the pure N_2 curve with the Ni(cyclam) peak, whereas the contributions at 40 and 50 vol% require fitting of the Ni(cyclam)CO peak as well, following the procedure described in SI-3. An example of the deconvolution for the cathodic scan of the 20 vol% CO curve is presented in Figure 2b, which gives a fraction of 0.76 unbound Ni(cyclam) and 0.24 CO-bound Ni(cyclam), respectively.

The binding constant is derived from the equilibrium between the carrier and CO (eq 2), based on the fractions of CO-bound and unbound Ni(cyclam) and the CO concentrations in the gas feed (Figure 2c). Rewriting the binding constant to a linear form (eq 3) allows us to get the binding constant (K_{CO}) and number of CO bound to a single carrier (a) from the intercept and slope of a linear fit through the data, respectively.[18]

$$[Ni^I(cyclam)] + aCO \rightleftarrows [Ni^I(cyclam)(CO)_a] \quad (1)$$

$$K_{CO} = \frac{C_{carrier-CO_a}}{C_{carrier}\cdot C_{CO}{}^a} = \frac{Y}{X\cdot C_{CO}{}^a} \quad (2)$$

$$\log\left(\frac{Y}{X}\right) = a\cdot\log(C_{CO}) + \log(K_{CO}) \quad (3)$$

Here, K_{CO} is the binding constant, $C_{carrier\text{-}CO_a}$ and Y are respectively the concentration and fraction of the CO-bound carrier, $C_{carrier}$ and X are respectively the concentration and fraction of the unbound carrier, a is the number of CO that bind per carrier, and C_{CO} is the concentration of CO in the solution.

From the slope of the linear fit in Figure 2d, we obtain a = 1.5, which should represent the number of CO molecules bound to a carrier. Our DFT calculations suggest that a second CO binding to $[Ni^I(cyclam)(CO)]^+$ is not energetically favorable (SI-5), and we observe the appearance of only one new redox peak in the CVs when introducing CO (Figure 2a), which both suggest that just a single CO is binding to the

https://doi.org/10.1021/acsenergylett.5c04138
ACS Energy Lett. 2026, 11, 2229−2234

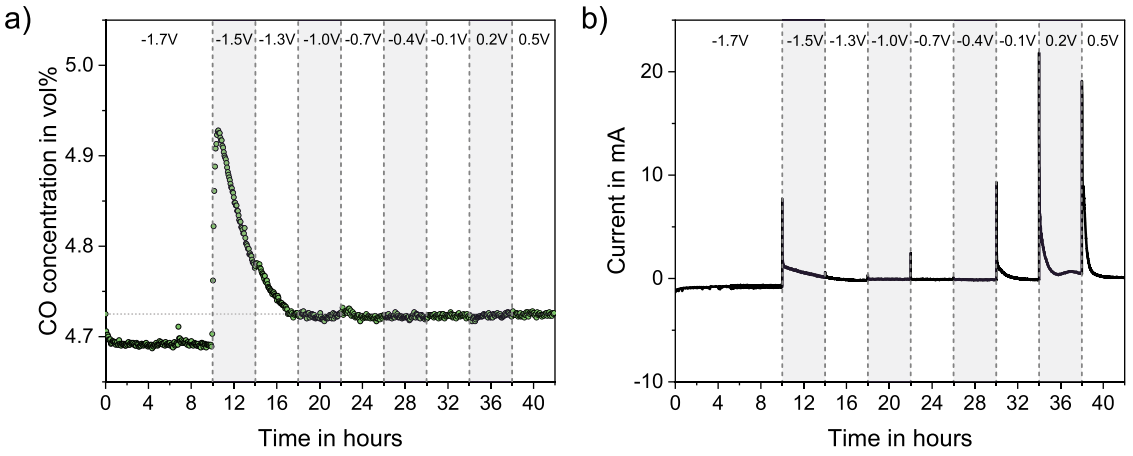


Figure 3. CO capacity measurement of 10 mM $[Ni(cyclam)]Cl_2$ and 0.1 M $TBAPF_6$ in a 4:1 acetonitrile−water solution. The CO feed was set to be 5 vol% of 10 mL min^{-1} in N_2. The potentials are versus ferrocene. (a) CO concentration profile in time. (b) Measured current at set potential in time.

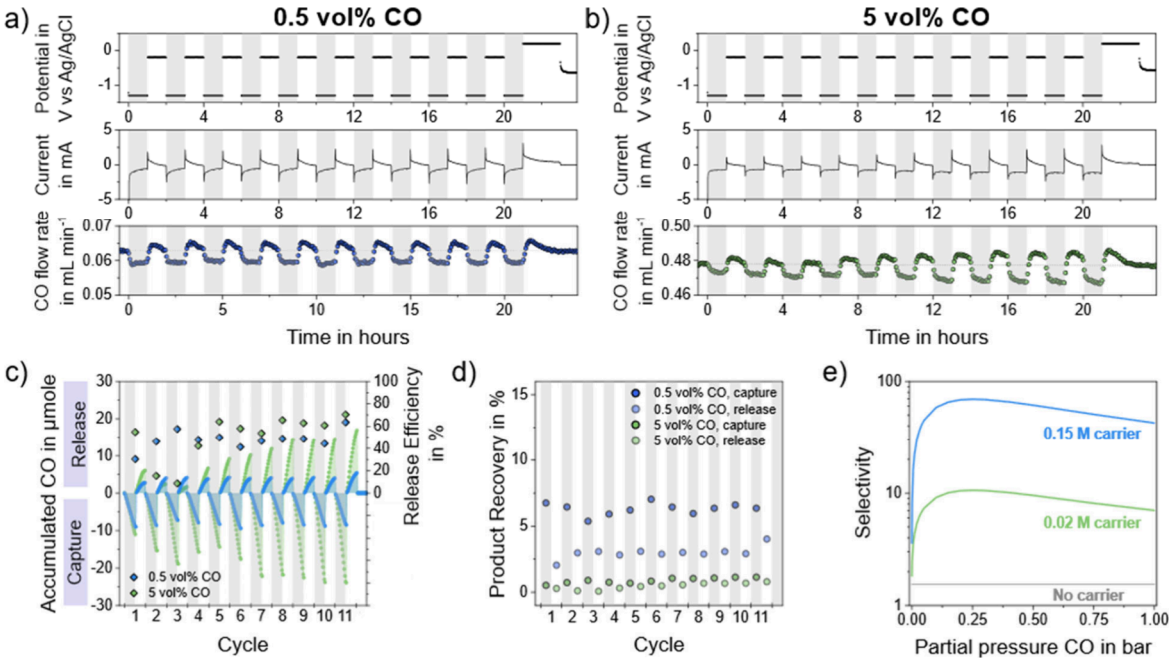


Figure 4. CO capture and release experiment of 20 mM $[Ni(cyclam)]Cl_2$ and 0.1 M $TBAPF_6$ in a 4:1 acetonitrile−water solution. The gas feed was 10 mL min^{-1} with 0.5 and 5 vol% CO in N_2. The gray area represents the capture part of the cycle, while the white part is the release part of the cycle. (a and b) Potential, current, and CO concentration data for 11 cycles with 0.5 vol% and 5.0 vol% CO in feed gas, respectively. (c) The accumulated amount of CO captured and released for the half-cycles and the release efficiency of each half-cycle. (d) The product recovery (defined as the percentage of the feed gas captured and/or released) of each half-cycle for the two CO concentrations. (e) Theoretical selectivity as a function of CO partial pressure for a carrier with a binding constant K_{CO} = 7000 M^{-1} and a = 1.5 at different carrier concentrations.

carrier. The slope, however, is sensitive to inaccuracies in the data. When the lowest concentration (5%), which might be affected by a change in the local concentration of CO during the measurement (SI-3), is ignored, the slope is 1.3 and even 1.16 at a faster scan rate (SI-6).

From the intercept, using all data at 50 mV s^{-1}, we obtain a binding constant of about 7 × 10^3 M^{-1}. We note that this binding constant is lower than the previously reported value for $[Ni^I(cyclam)]^+$ ($K_{CO} \approx 10^5$), but we deem our value more representative for flue gas applications as the previous work had fewer data points in the low-concentration regime (SI-6). The binding constant falls within the range of other materials' binding constant to CO (10^2−10^5).[15,16,19−21] In any case, this large value of 7 × 10^3 M^{-1} for the binding constant implies a strong capture potential, as the equilibrium lies toward the carrier with bound CO (eq 1).

We also assessed the effect of CO_2 in the $[Ni(cyclam)]Cl_2$ coordination, as blast furnace gas contains CO_2 and separating CO from CO_2 would allow for use of CO capture in CO_2 electrolysis. From CV curves in CO_2−N_2 and CO−CO_2−N_2, we conclude that $[Ni(cyclam)]Cl_2$ has minor (direct) affinity to CO_2, and with a different fingerprint than CO (SI-7).

Effect of Potential on the Release of CO

Capture and release of CO was performed in an H-cell. A 10 mL min^{-1} gas flow with 4.73 vol% CO (GC, set point was 5 vol%) was continuously fed to the working compartment (SI-2), and capture was achieved through activation of the carrier

https://doi.org/10.1021/acsenergylett.5c04138
ACS Energy Lett. 2026, 11, 2229−2234

by reduction to $[Ni^{I}(cyclam)]^{+}$ at −1.7 V vs ferrocene, resulting in a drop of measured CO concentration to just below 4.7 vol% (Figure 3a). This resulted in continuous capture for 10 h. After 10 h, the potential was increased in steps (of 4 h) to initiate the release of CO by oxidizing the carrier to $[Ni^{II}(cyclam)]^{2+}$ (regeneration). The first potential step (+0.2 V) to −1.5 V vs ferrocene is enough to release most of the previously captured CO, reaching a peak CO concentration of 4.93 vol% (feed still 4.73 vol%).

We note that the capture and release are very slow in the H-cell due to poor mass transfer. The oxidation and release span over the first two potential steps (−1.5 V and −1.3 V). The second potential step to −1.3 V vs ferrocene results in a small spike in current accompanied by a small bump in the CO concentration. Naturally, an increased rate of regeneration of the carrier results in an increased rate of release of CO, but the potential of −1.5 V vs ferrocene is already sufficient for the release of the captured CO, albeit slightly slower than at more positive potentials (see the slight bumps in Figure 3a at t = 14 h and t = 22 h). The latter corresponds to a potential of −0.7 V vs ferrocene, matching the CV's second oxidation peak that occurs in the presence of CO (Figure S11), which was suggested in previous work to be associated with stable Ni(0) carbonyl complexes.[12] Further oxidation to $[Ni^{III}(cyclam)]^{3+}$ around 0.2 V versus ferrocene does not result in additional release of CO and would therefore be a waste of energy.

Cyclic Capture and Release of CO by [Ni(cyclam)]Cl_2

For industrial application, a high recovery (>90%) is desired. When an absorption column and high recovery are visualized, the final stage of the gas feed has a low concentration, which is likely the most challenging condition for separating CO from N_2. To emulate the absorption and desorption for these low CO concentrations, we performed cyclic capture and release experiments using mix gas with 5 and 0.5 vol% CO in N_2 (Figure 4), with a half-cycle duration of 1 h (SI-2). A capture and release potential of −1.7 and −0.6 V vs ferrocene was used to ensure the release of all of the CO and prevent the deactivation of carrier material through irreversible binding.

The obtained CO flow rate at the outlet shows repeated capture and release over 11 cycles, with the 11th cycle releasing at a more positive oxidation potential (−0.2 V vs ferrocene). During the first four cycles, the system develops toward stable capture and release, with current efficiencies up to 100% for release in 5% CO and approximately 30% for capture and release in 0.5% CO (SI-13). As the carrier material is naturally primarily in the low-affinity state ($[Ni^{II}(cyclam)]^{2+}$), initially, more carrier material is being reduced than oxidized. This results in more capture of CO than release of CO and is represented by low release efficiencies (RE, defined as the percentage of captured CO being released in the next half-cycle) for the first four cycles (Figure 4c). A more positive release potential increases the release rate and release efficiency of CO (cycle 11 in Figure 4c), albeit at the expense of the current efficiency (SI-13).

After the initial cycles, the process seems to stabilize and shows cyclability for up to 10 cycles. The absolute amounts of CO absorbed are low (10−20 μmol per cycle), which can be attributed to the slow mass transport inside the H-cell. The concentration of freely soluble CO in an acetonitrile−water mixture is extremely low (~0.3 mM at P_{CO} = 0.05 bar), which causes the mass transport limitation. This is also visible in a faster decay in the current density compared to the sorption rates (SI-14). Implementation would require engineering toward increased absorption rates and electrochemical regeneration of the carrier, for example, through absorption columns and flow cell reactors. Also, practical operation should consider more narrow potential windows. Figure 3 suggests that switching between −1.7 V and −1.5 V vs ferrocene is even sufficient, which would lead—including Ohmic losses for an optimized system—to a rough estimated energy consumption of 150 kJ mol^{-1} (=1.5 kWh kg^{-1}) for an optimized flow cell reactor (SI-15).

We like to highlight the power of the high binding constant toward CO; with $K = 7 \times 10^3$ M^{-1} and a = 1.5 we estimate that the CO/N_2 selectivity is up to 70 for a carrier concentration of 0.15 M (Figure 4e), with commercial adsorbents ranging between 20 and 25 (SI-16).[4] As a result, the material is capable of separating CO from low-concentration streams, which proves especially challenging for existing separation technologies such as pressure swing sorption and cryogenic distillation.[4] A high binding constant can yield relatively high product recoveries (PRs) at low concentrations. Also here, the product recovery, defined as the percentage of the feed gas captured and/or released, is higher for the lower CO partial pressure (Figure 4d). The capability for capturing CO even at very low concentrations demonstrates the opportunities for electrochemically mediated separation of CO from industrial waste gases for carbon circularity.

In conclusion, we have demonstrated electrochemically mediated separation of carbon monoxide from nitrogen using [Ni(cyclam)]Cl_2 as the carrier material. Cyclic voltammetry measurements show a positive shift in the redox potential, indicating that the carrier has a higher binding affinity to CO in the 1+ oxidation state than the 2+ oxidation state, which is leveraged for the electrochemically mediated absorption of CO. The binding constant was estimated to be around 7×10^3 M^{-1} through deconvolution of the contributions of carriers with and without CO for the CV curves. We demonstrate that the material is capable of cycled capture and release of CO from 0.5 and 5 vol% CO streams, reaching a relatively stable operation after >4 cycles. A potential difference of 0.2 V is sufficient to switch between the capture and release of CO. Although the captured amount of CO is low in an H-cell, the high binding constant and good stability show potential for a CO separation system when optimizing mass transport and current density. With that, the electroactive carrier can concentrate CO through selective separation from nitrogen, offering a recycling opportunity for a currently lost feedstock that is generally emitted as CO_2.

■ ASSOCIATED CONTENT

Supporting Information

The Supporting Information is available free of charge at https://pubs.acs.org/doi/10.1021/acsenergylett.5c04138.

Material, experimental, and data processing procedures; additional CV measurements for $[Ni^{II}(cyclam)]^{2+}$/$[Ni^{III}(cyclam)]^{3+}$ redox couple, $NiCl_2$, and the carrier with CO_2; MFM data, current efficiency data, and CV measurements for capture and release experiments; more detailed discussions on the CV and the capture−release experiments, estimation of theoretical energy consumption, and implications of binding constant for separation selectivity; pictures of electrolyte solutions and H-cell (PDF)

https://doi.org/10.1021/acsenergylett.5c04138
ACS Energy Lett. 2026, 11, 2229−2234

AUTHOR INFORMATION

Corresponding Author

David A. Vermaas − *Department of Chemical Engineering, Delft University of Technology, 2629HZ Delft, Netherlands; e-Refinery Institute, 2628CB Delft, The Netherlands;* orcid.org/0000-0002-4705-6453; Email: d.a.vermaas@tudelft.nl

Authors

Christel I. Koopman − *Department of Chemical Engineering, Delft University of Technology, 2629HZ Delft, Netherlands; e-Refinery Institute, 2628CB Delft, The Netherlands*

Jelco Albertsma − *Department of Chemical Engineering, Delft University of Technology, 2629HZ Delft, Netherlands;* orcid.org/0000-0002-1842-8406

Monique A. van der Veen − *Department of Chemical Engineering, Delft University of Technology, 2629HZ Delft, Netherlands;* orcid.org/0000-0002-0316-4639

Complete contact information is available at: https://pubs.acs.org/10.1021/acsenergylett.5c04138

Notes

The authors declare no competing financial interest.

ACKNOWLEDGMENTS

This publication is part of Target 4 of the TTW Perspectief research programme ReCoVR: Recovery and Circularity of Valuable Resources (P19-20), which is (partly) financed by the Dutch Research Council (NWO). This work used the Dutch national e-infrastructure with the support of the SURF Cooperative using grant no. EINF-11304.

REFERENCES

(1) Bierhals, J. *Carbon Monoxide*; Wiley, 2001.

(2) Santos, S.; Hooey, L.; Boden, A.; Larsson, M.; Knights, M.; Johns, J.; Abraham, V.; Tobiesen, A.; Hoff, K. A.; Haugen, G. et al. *Iron and steel CCS study (techno-economics integrated steel mill)*; IEAGHG, 2013.

(3) Kennedy, E.; Sabag, O.; Gladek, E.; Thorin, T.; Moroney, M.; Schlueter, L.; Winkelman, J.; de Jong, W.; Heeres, E.; Graaf, G. *CORESYM: Carbon-monoxide re-use through industrial symbiosis between steel and chemical industries*; Metabolic, 2017.

(4) Ma, X.; Albertsma, J.; Gabriels, D.; Horst, R.; Polat, S.; Snoeks, C.; Kapteijn, F.; Eral, H. B.; Vermaas, D. A.; Mei, B.; et al. Carbon monoxide separation: past, present and future. *Chem. Soc. Rev.* **2023**, *52*, 3741−3777.

(5) Arvola, J.; Harkonen, J.; Mottonen, M.; Haapasalo, H.; Tervonen, P. Combining steel and chemical production to reduce CO_2 emissions. *Low Carbon Economy* **2011**, *2* (3), 115.

(6) James, J.; Lucking, L. E.; van Dijk, H. A. J.; Boon, J. Review of technologies for carbon monoxide recovery from nitrogen-containing industrial streams. *Frontiers in Chemical Engineering* **2023**, *5*, 01.

(7) Lu, E.; Atkinson, B. E.; Wooles, A. J.; Boronski, J. T.; Doyle, L. R.; Tuna, F.; Cryer, J. D.; Cobb, P. J.; Vitorica-Yrezabal, I. J.; Whitehead, G. F. S.; et al. Back-bonding between an electron-poor, high-oxidation-state metal and poor π-acceptor ligand in a urnaium-(v)-dinitrogen complex. *Nat. Chem.* **2019**, *11*, 806−811.

(8) Nowaczyk, A.; Kowalska, M.; Nowaczyk, J.; Grzesk, G. Carbon monoxide and nitric oxide as examples of the youngest class of transmitters. *International Journal of Molecular Sciences* **2021**, *22*, 6029.

(9) Voskian, S.; Hatton, T. A. Faradaic electro-swing reactive adsorption for CO2 capture. *Energy Environ. Sci.* **2019**, *12*, 3530−3547.

(10) Diederichsen, K. M.; Liu, Y.; Ozbek, N.; Seo, H.; Hatton, T. A. Toward solvent-free continuous-flow electrochemically mediated carbon capture with high concentration liquid quinone chemistry. *Joule* **2022**, *6*, 221−239.

(11) Mutch, G. A. Electrochemical separation processes for future societal challenges. *Cell Reports Physical Science* **2022**, *3*, 100844.

(12) Froehlich, J. D.; Kubiak, C. P. The homogeneous reduction of CO_2 by $[Ni(cyclam)]^+$: increased catalytic rates with the addition of a CO scavenger. *J. Am. Chem. Soc.* **2015**, *137* (10), 3565−3573.

(13) Froehlich, J. D.; Kubiak, C. P. Homogeneous CO_2 reduction by Ni(cyclam) at a glassy carbon electrode. *Inorg. Chem.* **2012**, *51* (7), 3932−3934.

(14) Gagne, R. R.; Allison, J. L.; Ingle, D. M. Unusual structural and reactivity types for copper(I). Equilibrium constants for the binding of monodentate ligands to several four-coordinate copper(I) complexes. *Inorg. Chem.* **1979**, *18* (10), 2767−2774.

(15) Mu, X. H.; Kadish, K. M. Oxidative electrochemistry of cobalt tetraphenylporphyrin under a CO atmosphere. Interaction between carbon monoxide and electrogenerated $[(TPP)Co]^+$ in nonbonding media. *Inorg. Chem.* **1989**, *28*, 3743−3747.

(16) Swistak, C.; Kadish, K. M. Electrochemistry of iron porphyrins under a CO atmosphere. Interactions between CO and pyridine. *Inorg. Chem.* **1987**, *26*, 405−412.

(17) Fujihira, M.; Suga, K. Electrocatalytic reduction of CO_{-2-} by nickel(II)cyclam. Study of the reduction mechanism on mercury by cyclic voltammetry, polarography and electrocapillarity. *Journal of Electroanalytical Chemistry and Interfacial Electrochemistry* **1990**, *292* (1-2), 199−215.

(18) Prinz, H. Hill coefficients, dose-response curves and allosteric mechanisms. *J. Chem. Biol.* **2010**, *3*, 37−44.

(19) Terry, P. A.; Walis, H. J.; Noble, R. D. Electrochemically modulated complexation process for gas removal and concentration. *AiChE Journal* **1995**, *41* (12), 2556−2564.

(20) Furenlid, L. R.; Renner, M. W.; Szalda, D. J.; Fujita, E. EXAFS studies on nickel(II), nickel(I), and Ni(I)-CO tetraazamacrocycles and the crystal structure of (5,7,7,12,14,14-hexamethyl-1,4,8,11-tetraazacyclotetradeca-4,11-diene)nickel(I) perchlorate. *J. Am. Chem. Soc.* **1991**, *113* (3), 883.

(21) Gagne, R. R.; Ingle, D. M. One-electrond-reduced nickel(II)-macrocyclic ligand complexes. Four-coordinate nickel(I) species and nickel(II)-ligand radical species which form paramagnetic, five-coordinate nickel(I) adducts. *Inorg. Chem.* **1981**, *20* (2), 420.